"The Collaborative Science, Technology, and Applied Research (CSTAR) Program"

Title:

"Cooperative Research with the National Weather Service on Cool- and Warm-Season Precipitation Forecasting over the Northeastern United States"

University: University at Albany

Name of University Researchers Preparing Report: Lance F. Bosart and Daniel Keyser

NWS/AFWA/Navy Office: National Weather Service, Albany, New York

Name of NWS/AFWA/Navy Researcher Preparing Report: Raymond O'Keefe

National Oceanic and Atmospheric Administration Award Number: NA01NWS4680002

Date: 27 May 2014

SECTION 1: Summary of Graduate Student Research Activities

(a) Northeast Cool-Season Cyclones Associated with Significant Upper-Level Easterly Wind Anomalies (Adrian Mitchell)
Focal Point: Neil Stuart, National Weather Service, Albany, NY

Research Summary (1 November 2013 – 30 April 2014):

Northeast cool-season cyclones can vary in track, duration, intensity and predictability. A category of these cyclones can be defined as those associated with strong upper-level zonal wind anomalies ($\leq -3\sigma$) poleward of the primary surface low (< 1000 hPa). These events tend to feature an upper level cutoff circulation with a deep, slow moving surface low. In many cases prolonged low-level northwesterly flow can interact with the complex topography of the northeast U.S. creating mesoscale orographic forcing for ascent. In the winter of 2010, two of these events, both associated with upper-level easterly jet streaks and low-level northerly warm-air advection, impacted the northeast U.S. These cyclones produced historic snowfall amounts as a result of orographic enhancement and were poorly forecast by numerical models. The anomalous nature of these types of events can lead to a decrease in predictability and a lack of situational awareness from an operational forecasting perspective. The opportunity exists to explore cyclones of a similar nature through a climatological and composite analysis, with a concentration on synoptic scale forcing features. 78 cyclone events have been identified between 1950-2010 using the NCEP/NCAR Reanalysis dataset.

Recent work has focused on classifying the 78 cyclone events based on synoptic structure. Cyclone events displaying a 300-hPa easterly jet streak (≥ 30 m s^{-1}) poleward of the surface low *and* 850-hPa northerly warm-air advection west of the surface low were classified as Easterly Jet Streak **(EJS)** events. To be considered an EJS event: 1) the 300-hPa jet streak core must have a primary easterly component and 2) the 850-hPa wind must have a primary northerly component and display warm-air advection (WAA). Remaining events were classified as either **open** or **cutoff** based on the configuration of the 300-hPa height field. To be considered a 'cutoff', there must be a 60 m height rise in all directions from center of the 300-hPa circulation. The grids for each cyclone were averaged and shifted to the centroid of all cyclones to create cyclone-relative composites for each category.

Figure 1 shows cyclone-relative composites for EJS, open and cutoff events. EJS events tend to be associated with a deep, closed 500-hPa vortex embedded in a negatively tilted long wave trough. A 60 kt 300-hPa easterly jet streak can be seen spanning northern Maine and southern Quebec, with favorable quasi-geostrophic (QG) forcing for ascent in the equatorward exit region over northern New England. High precipitable water (PW) values exist in a corridor wrapping cyclonically around the 500-hPa closed low with an apex over northern New England. The EJS composite surface cyclone is 982 hPa located just downstream of a negatively tilted 850-hPa thermal trough. High low-level relative humidity (RH) values exist over northern New England in a region associated with 850-hPa wrap around WAA. Orographic precipitation enhancement is likely in a region of northerly and northwest low-level flow in the Adirondack and Green mountain ranges.

Cutoff events are associated with a less intense 500-hPa vortex also embedded in a negatively tilted long wave trough. At 300 hPa a 60 kt southerly jet streak is located east of Boston, MA with QG forcing for ascent over much of New England in the left exit region of the jet. A high PW corridor is wrapping into eastern New England with an apex over southeast Maine. The cutoff composite surface cyclone is 988 hPa located over southern New England. The orientation of the 850-hPa wind and potential temperature fields indicates strong WAA and QG forcing for ascent over northern New England, coincident with high low-level RH values. Orographic precipitation enhancement is likely to the west of the surface cyclone in a region low-level northwesterly flow.

Open events are associated with a negatively tilted 500-hPa wave containing one closed height contour; the composite 500-hPa vorticity maximum is slightly weaker than in EJS and cutoff events as a result. Highly amplified upper-level flow exists over northeast North America with coupled 300-hPa jet streaks over the northwest Atlantic and east-central Quebec. Favorable QG forcing for ascent exists in northeast New England where the left exit and right entrance regions of the jet streaks overlap. High PW values collocated with a 30-40 kt low-level jet favors heavy precipitation in parts of eastern New England. The open composite surface cyclone is 990 hPa and is just downstream of 850-hPa thermal trough. The 850-hPa isentropes are meridionally oriented over much of New England indicative of the strong WAA to the north and east of the cyclone. High RH also exists to the north and east of the cyclone center, thus heavy precipitation is favored in this region. There is less of a signature for orographic enhancement due to lower RH values and weaker northwesterly winds to the west of the surface cyclone.

The three flavors of events identified can also be regarded as three stages of cyclone progression. The first stage consists of little to no wrap-around low-level WAA and no upper-level easterly jet streak, however strong forcing exists to the north and east of the cyclone (open events). The second stage shows more significant low-level wrap-around WAA and a developing easterly jet streak. This stage also consists of a closed 500-hPa vortex (cutoff events). The third stage now has significant low-level wrap around WAA and a well-defined upper-level easterly jet streak (EJS events). A checklist is currently being developed to help forecasters define what stage of progression the cyclone is at, and if it is likely to continue progressing or decay.

A climatological analysis has also been performed to more fully understand the frequency of these cyclone events and their relation to teleconnection patterns. Figure 2 shows the monthly and decadal cyclone frequencies as well as the cyclone intensity and events relative to Artic Oscillation (AO) value from 1950-2010. It is apparent that cyclone events occur throughout the cool-season with a maximum in December and April. The EJS events tend to be associated with stronger cyclones than open and cutoff events. When looking at events relative to AO value, EJS events appear to occur when the AO is significantly negative. Open and cutoff events also occur when the AO is predominately negative indicative of a strong upper-level blocking regime over the North Atlantic and a weak mid-latitude jet stream. A meridional flow pattern is necessary for the development of these three classifications of cyclones, so a rapidly declining AO index is warning signal for event occurrence.

Future work will include a continuation of case studies regarding four recent cyclone events. Two EJS cases, one open, and one cutoff case will undergo synoptic and mesoscale analysis to investigate primary forcing mechanisms. For the two EJS cases, WRF-ARW simulations have been performed and will continue to be analyzed in hopes of understanding the effects of topography during these cyclone events. Conceptual models will also be developed to aid operational forecasters and increase situational awareness when forecasting these cyclone

events. This research will culminate in the delivery of a M.S. thesis by 31 August 2014.

National Weather Service Interactions:

Communication between Adrian Mitchell (UAlbany) and Neil Stuart (WFO Albany) has been accomplished through meetings at the Albany NWS forecast office and through e-mail. Input from Neil Stuart regarding case studies and compositing methods has been useful in the development of this research. Continued collaboration will be necessary in order to optimize the usefulness of conceptual models and checklists from an operational forecasting perspective.

Publications and Workshop Submissions:

A poster devoted to the latest research was presented at the 94th Annual Meeting of the American Meteorological Society on 6 and 7 February 2014. The poster consisted of research methodology and the latest composite and climatological results. The feedback received at this conference helped facilitate improvements to the composite analysis methods and event climatology overview.

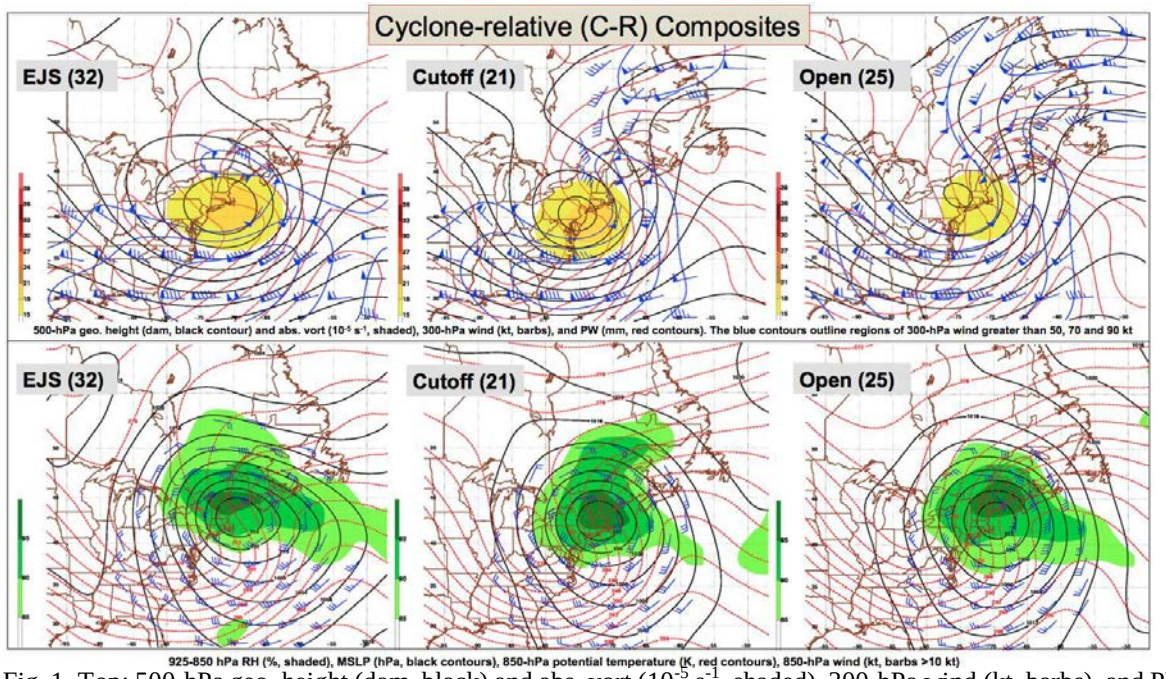

Fig. 1. Top: 500-hPa geo. height (dam, black) and abs. vort (10^{-5} s^{-1}, shaded), 300-hPa wind (kt, barbs), and PW (mm, red). The blue contours outline regions of 300-hPa wind greater than 50, 70 and 90 kt. Bottom: 925-850 hPa RH (shaded), MSLP (hPa, black), 850-hPa potential temperature (K, red), and 850-hPa wind (kt, barbs >10 kt)

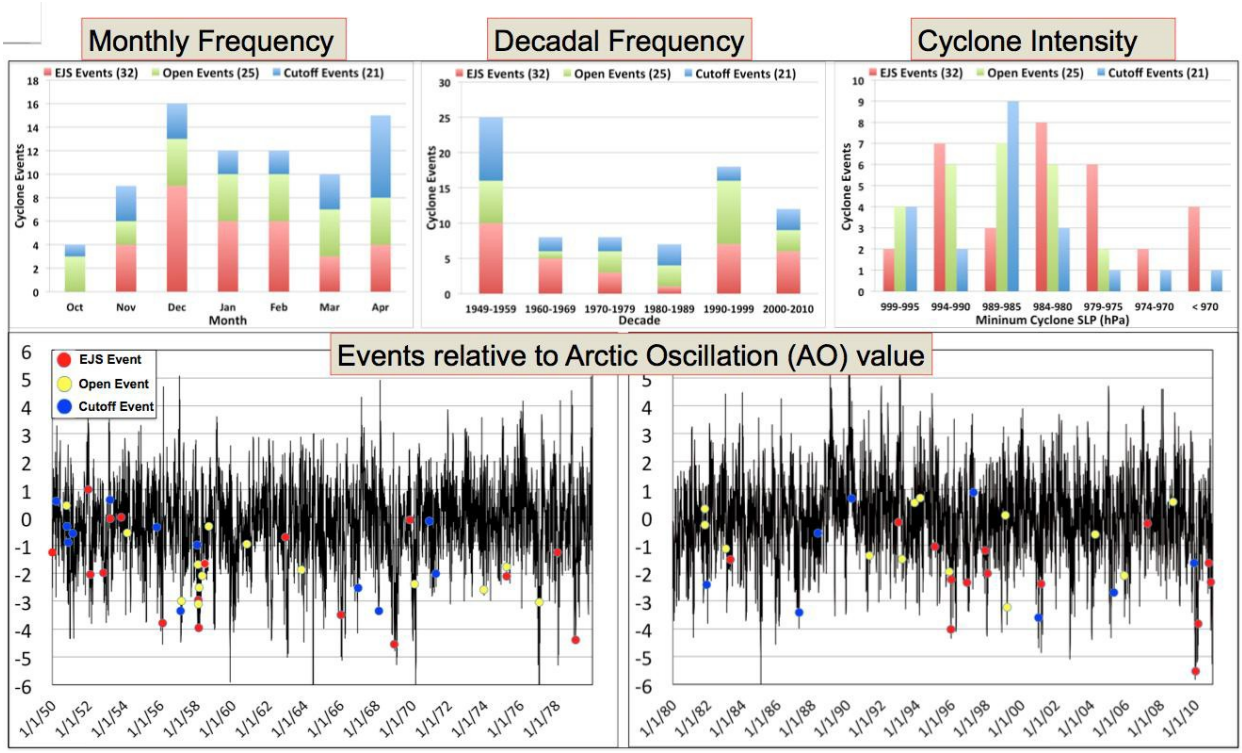

Fig. 2. Climatological data for three classifications of cyclones associated with upper-level zonal wind anomalies ≤ -3σ.

(b) Dynamical and Thermodynamic Processes Contributing to Thundersnow (Kyle Meier)
Focal Point: Michael Jurewicz, National Weather Service, Binghamton, NY

Research Summary (1 November 2013 – 30 April 2014):

In the recent phase of this CSTAR project, event-centered composites were constructed in order to determine the average dynamical and thermodynamic processes contributing to thundersnow in association with Nor'easter and lake effect events. First, METAR observations were scanned for all reports of thundersnow over the Northeast U.S. during the 1994–2011 cool season months (October–April). Archived surface maps, radar data, and NLDN observations were then used to categorize the reports based on event type. Only Nor'easter and lake effect events were queried for further analysis. A Nor'easter event was defined as thundersnow occurring in association with a costal cyclone that underwent significant development and attained maximum intensity near New England and the Maritime Provinces. A lake effect event was defined as a continental polar airmass moving over Lake Erie or Lake Ontario, extracting heat and moisture, and resulting in snowfall and lightning downwind of the lakeshore.

The aforementioned scanning process produced the distribution of thundersnow events shown in Fig. 1. An early cool-season bias is evident in the lake effect events (N=21), consistent with the fact that warmer lake-surface temperatures allow for greater convective cloud depths. A late cool-season bias is evident in the Nor'easter events (N=31). This result is likely due to the propensity for surface temperatures to be too warm to support frozen precipitation when lightning occurs in association with Nor'easters during the earliest cool-season months. Upon

categorizing the thundersnow events, composite analyses were constructed using the 0.5° Climate Forecast System Reanalysis data. All events were shifted to a central location and then diagnostic fields were averaged across member events. Before shifting the grids, each location for the Nor'easter events was defined as the surface cyclone center and each location for the lake effect events was defined as the snowband centroid. The time of each event was defined as the six-hourly (0000, 0600, 1200, or 1800 UTC) time in which there was a maximum in observed lightning.

Composite results for the Nor'easter events show that thundersnow tends to occur in the northwestern quadrant of a 990 hPa surface cyclone. The surface cyclone resides in the left exit region of a 250 hPa jet streak (60 m s^{-1}), with a coupled jet signature also evident. At 500 hPa, a short-wave disturbance and associated vorticity maximum (32 x 10^{-5} s^{-1}) reside upstream of the surface cyclone, providing a favorable setup for cyclogenesis and large-scale ascent over the region in which thundersnow occurs. At 700 hPa, a closed 280 dam low and near-saturated conditions exist over the region where thundersnow occurs. This closed midlevel circulation often supports deformation, frontogenesis, and associated mesoscale snowbanding. Therefore, there may be a connection between mesoscale snowbands and thundersnow. Strong warm air advection is evident in the lower troposphere as well, providing an additional mechanism for synoptic-scale forcing. The overall synoptic-scale forcing for ascent is highlighted by a maximum in Q-vector convergence (21 x 10^{-16} K m^{-2} s^{-1}) over the region where thundersnow occurs. From a mesoscale perspective, thundersnow associated with Nor'easter events tends to occur in a region of strong 700 hPa frontogenesis and 700–500 hPa saturation equivalent potential vorticity (EPV*) values near zero. A composite sounding for the location where thundersnow occurs depicts 0 J kg^{-1} of CAPE. However, individual case studies have suggested that the thundersnow environment often contains at least modest amounts of CAPE (< 300 J kg^{-1}). The composite sounding also reveals relatively steep midlevel (700–500 hPa) lapse rates that approach moist adiabatic (6.4°C km^{-1}). These steep lapse rates intersect both the mixed-phase and dendritic growth zone regions of the atmosphere. Strong updrafts through the mixed-phase region are necessary for electrical charge separation, and strong updrafts through the dendritic growth zone often result in high snowfall rates and accumulations.

Composite results for the lake effect events show that thundersnow tends to occur to the south of a relatively weak 1004 hPa surface cyclone and on the cyclonic side of a 250 hPa jet streak (50 m s^{-1}). Although the signal is less robust than with Nor'easter events, there is evidence of a 500 hPa short-wave disturbance upstream of the location where thundersnow tends to occur. This result is important because cyclonic vorticity advection above the capping inversion can raise the inversion level over the boundary layer, enhancing lake effect snowfall, and promoting lightning by allowing for deeper convection. At 700 hPa, a 284 dam open wave structure and near-saturated conditions exist over the region where thundersnow occurs. With a notable absence of Q-vector convergence, there is considerably less synoptic-scale forcing associated with lake effect events as compared to the Nor'easter events. However, lake effect thundersnow events are accompanied by strong cold air advection in the lower levels of the troposphere, resulting in a significant amount of instability. Lapse rates steepen to greater than most adiabatic (6.5°C km^{-1}) from the surface up to ~500 hPa, implying that heat and moisture form the lake surface can easily mix to high levels in the troposphere, producing deep wintertime convection. Similar to the Nor'easter thundersnow events, lake effect thundersnow events exhibit large upward vertical velocities intersecting the mixed-phase and dendritic growth zone regions, suggesting lightning generation and high snowfall rates. Overall, the composite results are useful

in illustrating the synoptic-scale environment in which thundersnow is embedded. However, details regarding mesoscale processes and instability regimes can be lost when averaging so many events. The ensuing paragraphs will summarize two case studies representative of Nor'easter and lake effect events, respectively.

A Miller Type-A Nor'easter produced significant snowfall accumulations and lightning across parts of New England on 11–12 February 2006. New York City received an all-time record amount of snow (68 cm) and severe coastal impacts were felt in Massachusetts, as winds up to 52 knots produced storm surges of two to three feet. Overall, 27 NLDN lightning flashes were detected with this event, 3/27 (11%) of which were positive in polarity (Fig. 2). This event commenced with a relatively weak surface cyclone that brought accumulating snow to the southern Appalachians on 11 February. The surface cyclone then moved offshore before rapidly intensifying and merging with a northern stream system on 12 February.

A cross section taken through a cluster of lightning flashes depicts the instability and mesoscale features associated with this event. The cross section shows a band of moderate to strong frontogenesis from the surface to ~600 hPa, with a maximum value of 21 K $(100\ \mathrm{km})^{-1}$ $(3\ \mathrm{h})^{-1}$ centered around 775 hPa (Fig. 3a). Additionally, weakly negative EPV* values exist in the vicinity of the frontogenesis and beneath a region of implied instability. Since the saturation equivalent potential temperature contours are largely upright above the negative zone of EPV*, it is likely that conditional symmetric instability was released in this event. Finally, the highest values of upward vertical velocities intersect the mixed-phase region of the troposphere (Fig. 3b).

An early-season lake effect snowstorm hit the Buffalo, NY area on 12–13 October 2006. The storm was most unique in regards to its power outages and destruction of trees, directly due to its out-of-season factor. Heavy snow with snow-water equivalent values as low as 6:1 piled onto trees that were fully foliated, leading to significant damage. Overall, 217 NLDN lightning flashes were detected with this event, 42/217 (19%) of which were positive in polarity (Fig. 4). The synoptic-scale setup was highlighted by a surface cyclone that organized over Lake Superior and subsequently intensified as it tracked to the northeast. By 0000 UTC 13 October, the surface cyclone had deepened to 976 hPa and become well stacked from the surface to 300 hPa, providing for deep cyclonic flow over Lake Erie. Cold air advection in the lower troposphere increased 700–500 hPa lapse rates to around 7.0°C km^{-1} and lapse rates in the 1000–700 hPa layer were greater than 8.0°C km^{-1}.

A cross section taken through BUF at 2100 UTC 12 October reveals that the thundersnow occurred where weak to moderate low-level frontogenesis (below 800 hPa) coincided with saturation equivalent potential vorticity values as low as −0.75 PVU (Fig. 5). Saturation equivalent potential temperature decreased with height from the surface to ~775 hPa, suggesting that conditional instability was present in the lower troposphere. This conditional instability would have resulted in upright convection and subsequent vertical motions. A special sounding also valid at 2100 UTC 12 October estimates that ~287 J kg^{-1} CAPE was available for this event (Fig. 6). Additionally, an anomalously warm lake-surface temperature ~16°C and an 850 hPa temperature of −6°C, resulted in a $\Delta T_{\mathrm{sfc\text{-}850hPa}}$ of 22°C, greatly exceeding the well-accepted threshold of 13°C necessary for lake effect precipitation. An 850 hPa wind direction of 247° and weak directional shear throughout the troposphere was optimal for producing the intense, single-banded storm observed in this event. Finally, the −10°C isotherm was high enough off the ground (~1.9 km) that vertical motions in the lower troposphere could become of sufficient

intensity to separate charge and the entire mixed-phase region resided within the lake effect cloud layer (i.e., the layer bounded by the LCL and EL).

National Weather Service and Scientific Interactions:

Communication with Michael Jurewicz (WFO Binghamton) has occurred via email correspondence and will continue at the 2014 Spring CSTAR meeting. The author has continued to update Chris Melick (CIMMS Research Associate) on his research progress as well.

Publications and Conference Presentations:

39th Annual Northeastern Storm Conference, Rutland, VT, 7–9 March 2014
Oral Presentation: *Dynamical and Thermodynamic Processes Contributing to Thundersnow Events*
94th AMS Annual Meeting, Atlanta, GA, 2–6 February 2014
Poster Presentation: *Dynamical and Thermodynamic Processes Contributing to Thundersnow Events*

Northeast Regional Operational Workshop XIV, Albany, NY, 10–11 December 2013
Oral Presentation: *Regional Variability and Frequency of Thundersnow Events over the Contiguous U.S.*

Figures and Web Links:

Composite results for Nor'easter thundersnow events:
http://www.atmos.albany.edu/student/kmeier/charts/composites/Noreaster/

Composite results for lake effect thundersnow events:
http://www.atmos.albany.edu/student/kmeier/charts/composites/LakeEffect/

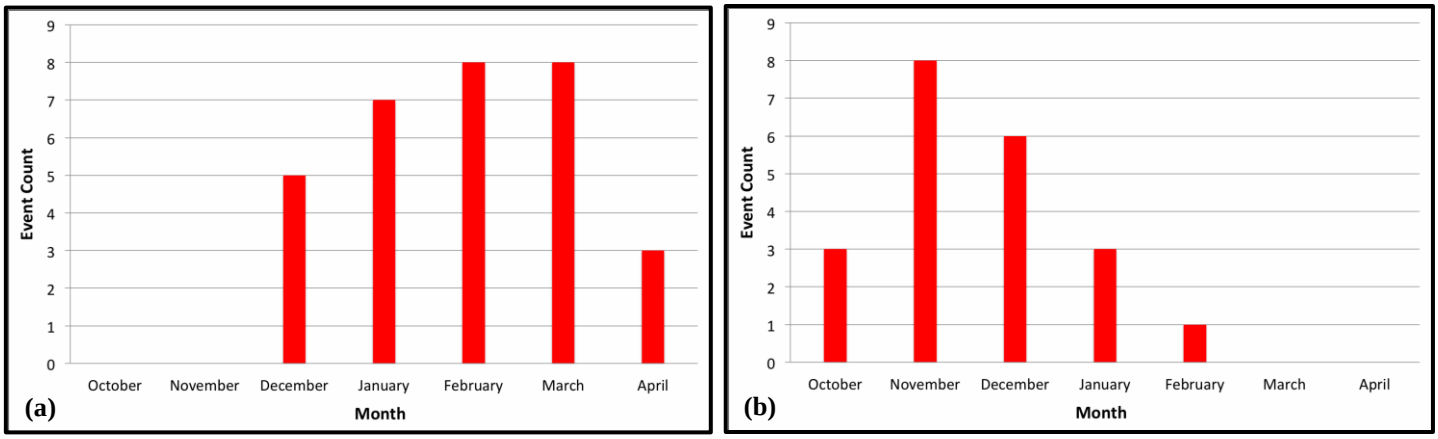

Fig. 1. Monthly distribution of thundersnow events over the Northeast U.S. for (a) Nor'easter events and (b) lake effect events

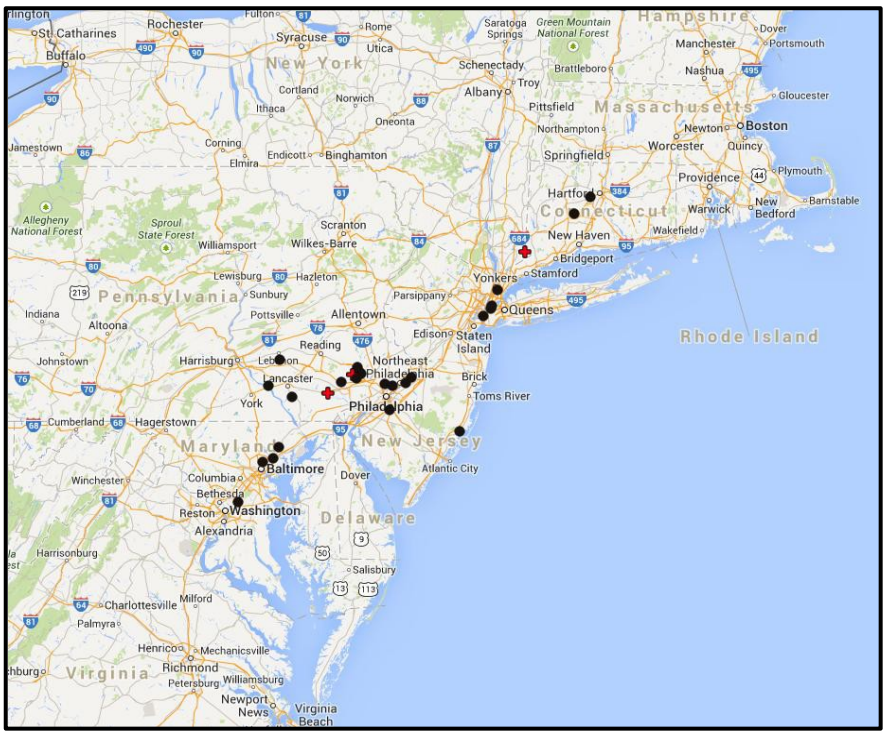

Fig. 2. NLDN lightning flashes (N=27) for 11–12 February 2006. Positive flashes are denoted by the red plus signs and negative flashes are denoted by the black dots.

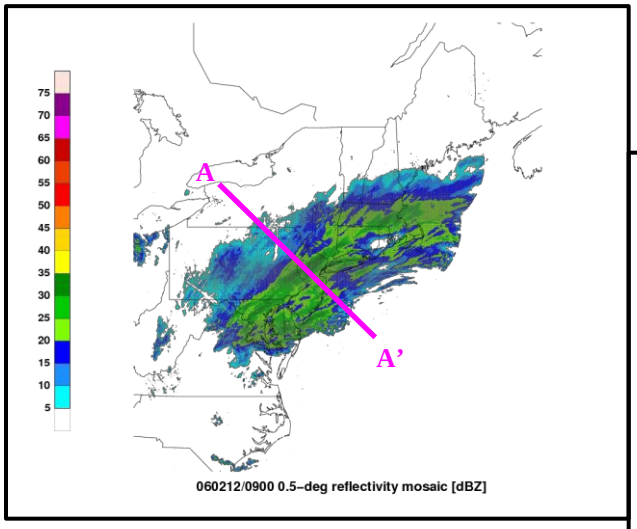

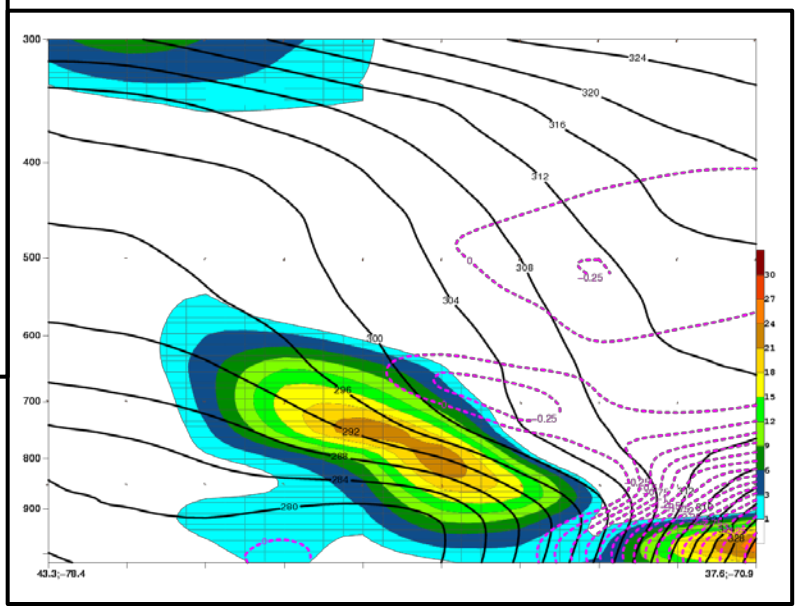

Fig. 3a. Vertical cross section from 43.3°N, −78.4°W (denoted A above) to 37.6°N, −70.9°W (denoted A' above) using RUC model data for 0900 UTC 12 February 2006. Shown are saturation equivalent potential temperature (black, every 4 K), frontogenesis [fill, every 3 K (100 km)$^{-1}$ (3 h)$^{-1}$], and saturation equivalent potential vorticity (magenta, negative values only, every 0.25 PVU). Cross section orientation is approximately normal to the 1000–500 hPa thermal wind.

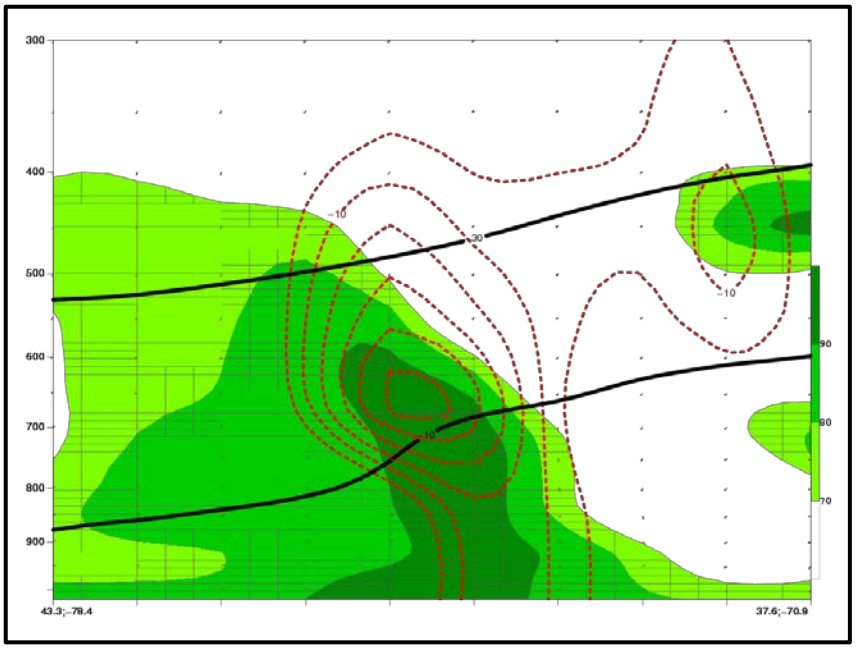

Fig. 3b. Vertical cross section showing relative humidity (every 10%, starting at 70%), upward vertical velocities (≤ −8 x 10^{-3} hPa s^{-1}), and the mixed-phase region (layer bounded by the −10°C and −30°C isotherms) of the troposphere. Cross section is valid at the same time and for the same location as in 3a.

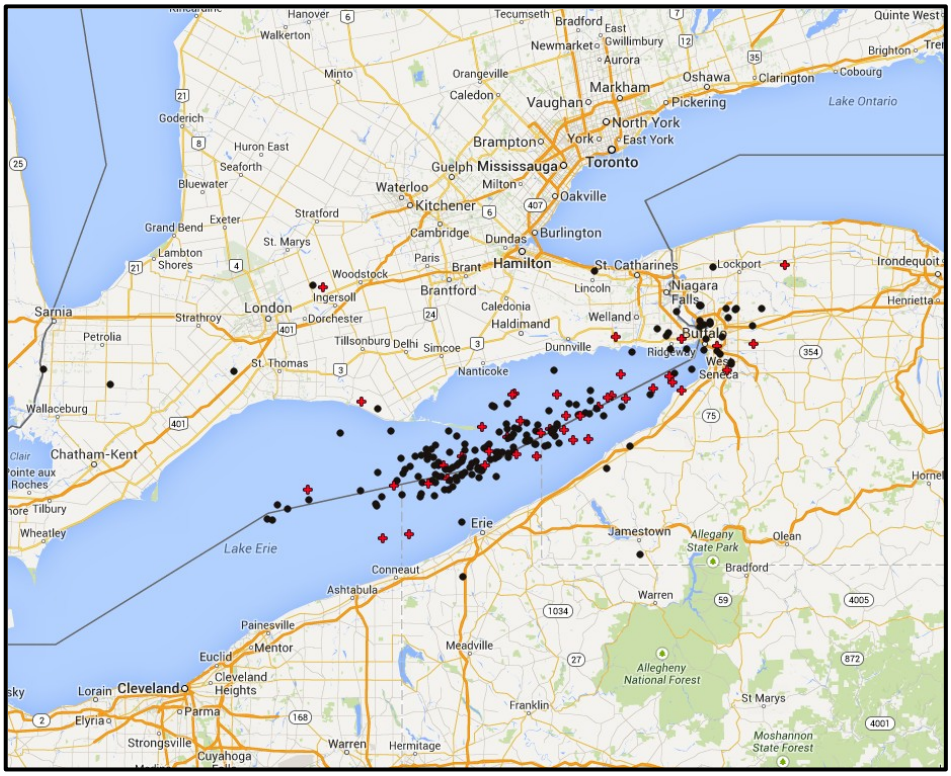

Fig. 4. NLDN lightning flashes (N=217) for 12–13 October 2006. Positive flashes are denoted by the red plus signs and negative flashes are denoted by the black dots.

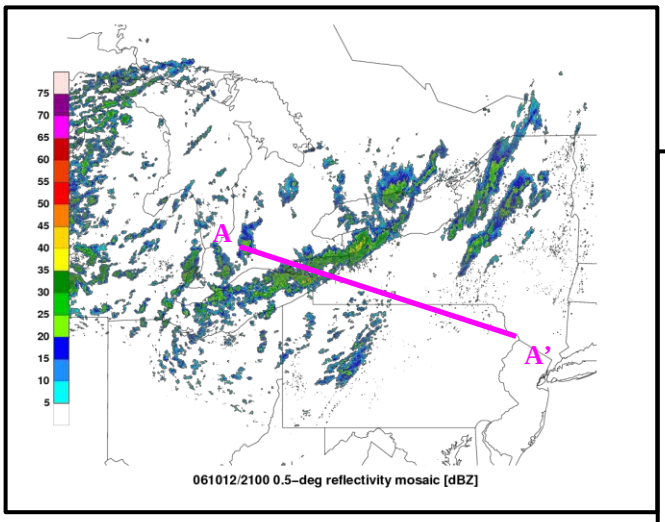

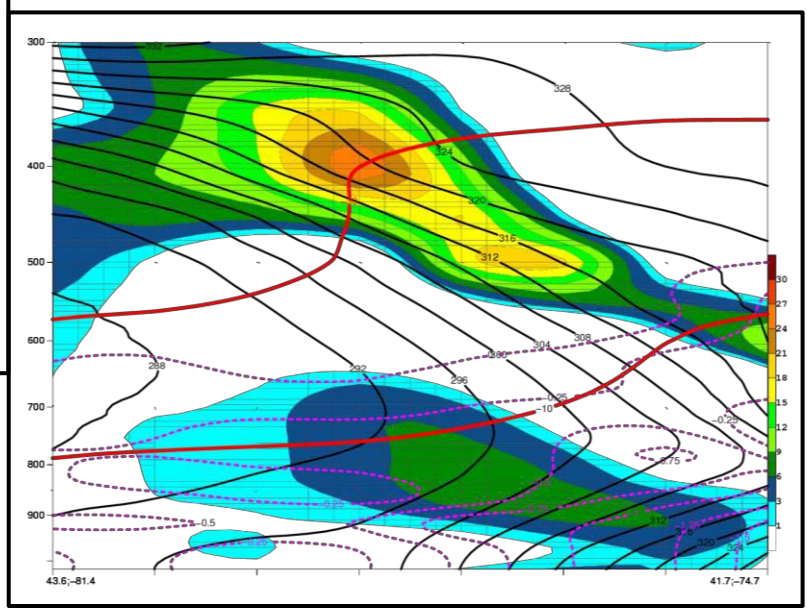

Fig. 5. Vertical cross section from 43.6°N, −81.4°W (denoted A above) to 41.7°N, −74.7°W (denoted A' above) using RUC model data for 2100 UTC 12 October 2006. Shown are saturation equivalent potential temperature (black, every 4 K), frontogenesis [fill, every 3 K (100 km)$^{-1}$ (3 h)$^{-1}$], and saturation equivalent potential vorticity (magenta, negative values only, every 0.25 PVU). Also shown is the mixed-phase region of the troposphere (highlighted in the red contours). Cross section orientation is approximately normal to the 1000–500 hPa thermal wind.

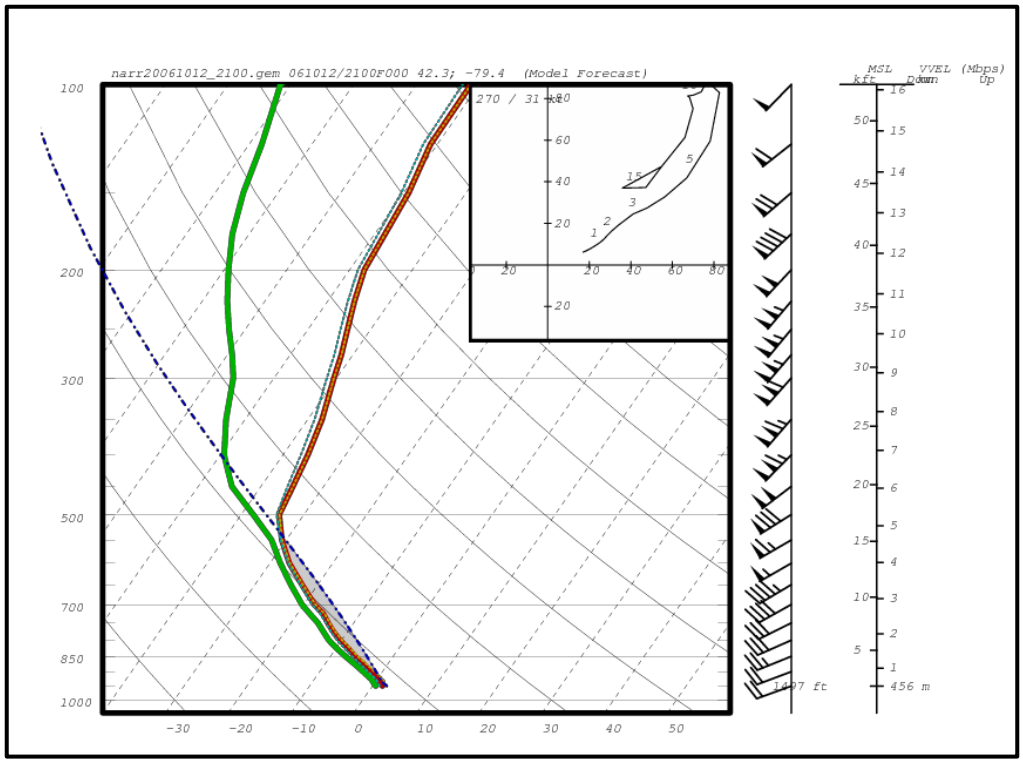

Fig. 6. Temperature and dewpoint profiles at BUF valid at 2100 UTC 12 October 2006, a time in which frequent lightning was observed in the Buffalo metropolitan area.

SECTION 2: Cumulative CSTAR Project Publications

a) **Theses completed:** Refer to

http://www.atmos.albany.edu/facstaff/kristen/CSTAR/CSTAR_CumulativePublications.pdf

b) **Preprints:** Refer to

http://www.atmos.albany.edu/facstaff/kristen/CSTAR/CSTAR_CumulativePublications.pdf

c) **Co-PI and/or student presentations:** Refer to

http://www.atmos.albany.edu/facstaff/kristen/CSTAR/CSTAR_CumulativePublications.pdf

Citations for March–April 2014:

Bosart, L. F., A. M. Bentley, and P. P. Papin, 2014. The uber jet and the widespread disruptive ice storm of 21–23 December 2013. Oral presentation at the 39th Annual Northeastern Storm Conference, 7–9 March, Rutland, VT.

Meier, K. J., D. Keyser, L. F. Bosart, and M. L. Jurewicz, Sr., 2014. Dynamical and thermodynamic processes contributing to thundersnow events. Oral presentation at the 39th Annual Northeastern Storm Conference, 7–9 March, Rutland, VT.

d) **CSTAR/COMET related refereed publications:**

http://www.atmos.albany.edu/facstaff/kristen/CSTAR/CSTAR_CumulativePublications.pdf

Kunkel et al. citation has been revised to show correct year of publication:

Kunkel, K. E., K. R. Thomas, H. Brooks, J. Kossin, J. H. Lawrimore, D. Arndt, L. F. Bosart, D. Changnon, S. L. Cutter, N. Doesken, K. Emanuel, P. Y. Groisman, R. W. Katz, T. Knutson, J. O'Brien, C. J. Paciorek, T. C. Peterson, K. Redmond, D. Robinson, J. Trapp, R. Vose, S. Weaver, M. Wehner, K. Wolter, and D. Wuebbles, 2013: Monitoring and understanding trends in extreme storms: State of knowledge. *Bull. Amer. Meteor. Soc.*, **94**, 499–514.

SECTION 3: NWS Perspective on CSTAR Progress (Warren Snyder). Refer to pp. 6–7 of CSTAR V six-month report dated 25 March 2014.

SECTION 4: Status of "Snyder Plan" Projects (Warren Snyder and Focal Points). Refer to pp. 7–10 of CSTAR V six-month report dated 25 March 2014.

SECTION 5: Computer and Technology Transfer Issues (David Knight)

Computing infrastructure continues to play an important part in this collaborative effort. Students are exposed to NWS facilities and software, and NWS staff has access to capabilities not available in the local office. Both groups benefit from this interaction and sharing of facilities. Several Sun workstations and PCs are available for use by CSTAR participants. Approximately 2 TB of disk space on the UAlbany Department of Earth and Atmospheric Science (DAES) Sun servers is dedicated to storing CSTAR related data and software. This disk space is available on all DAES workstations and provides a central location where both UAlbany and NWS personnel can store, process, and exchange large datasets. Each CSTAR student has a PC or Mac laptop, which enables them to take familiar computers with them when visiting NWS staff, and provides them ready access to the DAES UNIX machines. CSTAR Email lists originally created on the DAES computers at the beginning of the project have been superseded by the "map" list (map@listserv.albany.edu). The "map" list reaches a much larger audience (out of 410 members, roughly 1/4 are from NOAA), allowing discussion of CSTAR related research among many more people. Albany WSFO staff took the lead in maintaining content for the CSTAR webpage at http://cstar.cestm.albany.edu. The web page provides an additional mechanism for exchanging information and ideas. The WSFO also runs a CSTAR forum and discussion group at http://infolist.nws.noaa.gov/read/?forum=cstar_ne. The DAES web server (http://www.atmos.albany.edu) and ftp server (ftp://ftp.atmos.albany.edu) are being used to facilitate exchange of large datasets between CSTAR collaborators. The DAES computing resources are available for CSTAR related research including a Sun server (with 8 CPUs and
16GB RAM), a Linux server (with 16 CPUs and 128GB RAM) and two large network attached disk storage arrays (80 TB total usable space). While CSTAR money was not used for this, and the machines were not bought specifically for CSTAR use, they nonetheless directly benefit the CSTAR research by providing much faster servers for computation and storage space for commonly used datasets.

In addition to DAES, and NWS computing facilities, the formal CSTAR collaborative grant effort has allowed access to University Research Information Technology (RIT) services. In particular, Warren Snyder (SOO Albany WSFO) is using the RIT 144 CPU Linux cluster for Weather Research and Forecasting (WRF) model simulations. This computing facility allows him to perform computations not possible at the local office. The facility will be used to generate additional members for the collaborative ensemble, and to generate higher resolution runs for research purposes. So far this facility has been made available at no cost to the CSTAR project.